

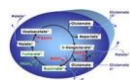


# High-resolution respirometry and coupling control protocol with intact cells: ROUTINE, LEAK, ETS, ROX

O2k-Workshop Report, IOC23, Schroecken, Austria.

Gnaiger E, Renner-Sattler K

**OROBOROS INSTRUMENTS Corp**  
high-resolution respirometry  
Schöpfstr 18, A-6020 Innsbruck, Austria  
[erich.gnaiger@oroboros.at](mailto:erich.gnaiger@oroboros.at); [www.oroboros.at](http://www.oroboros.at)  
Medical University of Innsbruck, Department of Transplant Surgery  
D. Swarovski Research Laboratory  
6020 Innsbruck, Austria



## Section

## Page

1. Introduction .....	2
2. Coupling control protocol, CCP .....	3
2.1. ROUTINE flux control ratio, ROUTINE/ETS ( $R/E$ ) .....	4
2.2. LEAK flux control ratio, LEAK/ETS ( $L/E$ ) .....	4
2.3. Net ROUTINE flux control ratio, netROUTINE/ETS ( $netR/E$ ) .....	5
3. The O2k-Workshop experiment .....	6
4. References .....	8
Supplement: Cell respiration, calibration and background correction .....	9

**Summary:** An experiment on cellular respiration is reported from an O2k-Workshop on high-resolution respirometry. Leukemia cells were incubated at a density of 1 million cells/ml in 2 ml culture medium in two O2k chambers operated in parallel. Cellular ROUTINE respiration,  $J_R$ , resulted in volume-specific oxygen consumption of  $20 \text{ pmol}\cdot\text{s}^{-1}\cdot\text{ml}^{-1}$ . Oxygen concentration changed by merely 6.4 and 6.5  $\mu\text{M}$  in the two O2k-Chambers over a period of 5 min ( $<1\%$  air saturation per minute). Inhibition by oligomycin ( $J_L$ ), and rotenone (residual oxygen consumption,  $J_{ROX}$ ; after uncoupling) reduced respiration to 5 and 1  $\text{pmol}\cdot\text{s}^{-1}\cdot\text{ml}^{-1}$ , while inducing the non-coupled state by FCCP revealed the capacity of the electron transfer system (ETS) at  $J_E$  of  $50 \text{ pmol}\cdot\text{s}^{-1}\cdot\text{ml}^{-1}$ . The ROUTINE flux control ratio,  $R/E$ , was 0.39 (uncoupling control ratio,  $UCR=E/R=2.6$ ), and the LEAK flux control ratio,  $L/E$ , was 0.09 ( $E/L=12.0$ ). This indicates tight

coupling of OXPHOS, and a large respiratory excess capacity over ROUTINE respiration. The net ROUTINE flux control ratio,  $netR=(R-L)/E$  was 0.30, indicating that 30% of ETS capacity was activated for ATP production.

Automatic correction for instrumental background amounted to 13% for ROUTINE respiration, but to >50% and 180% for  $J_L$  and  $J_{ROX}$ , respectively, illustrating the importance of real-time correction. The experiment illustrates the sensitivity and reproducibility of high-resolution respirometry with the OROBOROS Oxygraph-2k. Calibrations and routine corrections provide the basis of the high accuracy required for mitochondrial respiratory physiology. Real-time analyses were performed, combining high-resolution with instant diagnostic information. In this update graphs are presented illustrating some features of DatLab.

## 1. Introduction

Small changes in cellular respiration, minor alterations in respiratory control ratios, and minor differences in the respiratory effects of inhibitors may indicate significant mitochondrial defects, severe injuries of mitochondrial proteins or mtDNA, or decisive alterations in the state of mitochondrial signalling cascades. The standards set by the OROBOROS Oxygraph-2k for high resolution respirometry are required to resolve current scientific challenges in mitochondrial physiology and respiratory pathology.

Over a period of more than 10 years, high-resolution respirometry was developed, applied in many laboratories, and recently further advanced, leading to the state-of-the-art instrument – the OROBOROS Oxygraph-2k. The present application note is based on a demonstration experiment performed during a workshop and training course on high-resolution respirometry ([IOC23](#), Schröcken, March 2003). For the present updated report, files recorded with DatLab 3 were imported into the new DatLab version. The experiment is restricted to a single run in duplicate, using the two chambers of the Oxygraph-2k in parallel (Fig. 1). A demonstration experiment carried out during an introductory course does not achieve a statistically complete result nor do the data correspond to the standard of routine laboratory conditions. The results demonstrate, however, the high reproducibility and instrumental reliability in a routine application of high-resolution respirometry.

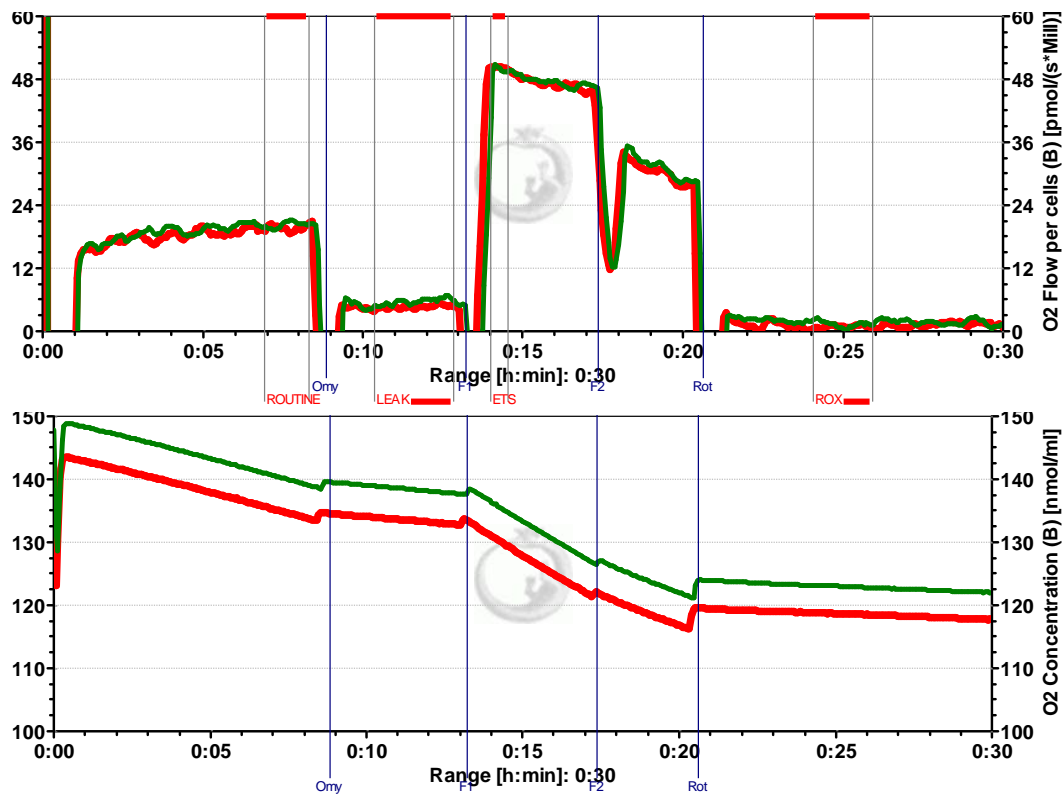


**Figure 1.** Traces of respiration A: O<sub>2</sub> flux, corrected for instrumental background; B: oxygen concentration in the two simultaneously operated Oxygraph-2k chambers. See Figure 2 for experimental details. DatLab file: 2003-03-29 O2k1-02\_Cells\_0809.DLD. Scaling of plots was edited after selecting the graph layout "07 Gr1-Flux Gr2-O<sub>2</sub> Conc".

## 2. Coupling control protocol, CCP

A suspension of lymphocytes in culture medium (RPMI) was added to the Oxygraph-2k chambers at a concentration of c.  $1 \cdot 10^6$  cells/ml. The coupling control protocol was applied to evaluate the cellular routine respiratory state, the mitochondrial coupling state, non-coupled respiratory capacity, and rotenone-insensitive or residual oxygen consumption. This protocol takes 30 min, including (1) a 10-min period of cellular ROUTINE respiration ( $J_R$ ; state *R*), reflecting the aerobic metabolic activity under routine culture conditions (with the physiological substrates in culture medium), (2) the oligomycin-inhibited LEAK respiration ( $J_L$ ; state *L*), which is caused mainly by compensation for the proton leak after inhibition of ATP synthase; (3) FCCP stimulated respiration, reflecting the electron transfer system (ETS) capacity at non-coupled respiration of intact cells ( $J_{E_i}$ ; state *E*); (4) rotenone- and (5) antimycin-inhibited respiration after sequential inhibition of Complex I and III ( $J_{ROX}$ ). Fluxes in states

$R$ ,  $L$  and  $E$  are corrected for  $J_{\text{ROX}}$ . All inhibitors and the uncoupler applied in this protocol are freely permeable through the intact plasma membrane and do not require, therefore, cell membrane permeabilization.

Depending on quantification of cellular mass, cell volume or number, respiratory flux per volume ( $J_{V,O_2}$ , per ml of cell suspension) is converted to an extensive quantity (flow;  $I_{O_2}$ , per cell or per million cells) or a cell size-specific quantity (flux;  $J_{O_2}$ , per cell protein or dry weight, cell volume). In addition to information on absolute respiratory fluxes, flux control ratios ( $FCR$ ) are derived from the present protocol (Fig. 1).

## 2.1. ROUTINE flux control ratio, ROUTINE/ETS ( $R/E$ )

The ratio of (coupled) ROUTINE respiration and (non-coupled) ETS capacity is the  $R/E$  flux control ratio ( $J_R/J_E$ ). The  $R/E$  ratio is an expression of how close ROUTINE respiration operates to the respiratory capacity of the ETS. The  $R/E$  ratio increases due to (i) high ATP demand and ADP-stimulated ROUTINE respiration, (ii) partial uncoupling, and (iii) limitation of oxidative capacity by defects of substrate oxidation and complexes of the ETS. The corresponding inverse ratio is the uncoupling control ratio, UCR, which can be seen as an index of ETS reserve capacity.

## 2.2. LEAK flux control ratio, LEAK/ETS ( $L/E$ )

The ratio of (non-coupled) LEAK respiration and (non-coupled) ETS capacity is the  $L/E$  flux control ratio ( $J_L/J_E$ ). LEAK respiration is measured as oligomycin-inhibited respiration in intact cells. Inhibition of ATP synthase exerts respiratory control on coupled OXPHOS, with the effect of an increased mitochondrial membrane potential and maximum proton leak or slip, which is compensated for by the LEAK respiration. In isolated mitochondria or permeabilized cells, LEAK respiration can be evaluated at defined adenylate concentrations: N, no adenylates, or T: minimum ADP concentration in the presence of ATP (Gnaiger 2012). Dyscoupling increases the  $L/E$  ratio. Importantly, an increased  $L/E$  ratio provides proof for dyscoupling only at constant ETS capacity. Alternatively, the  $L/E$  ratio may increase in normally coupled mitochondria if the respiratory capacity is diminished.

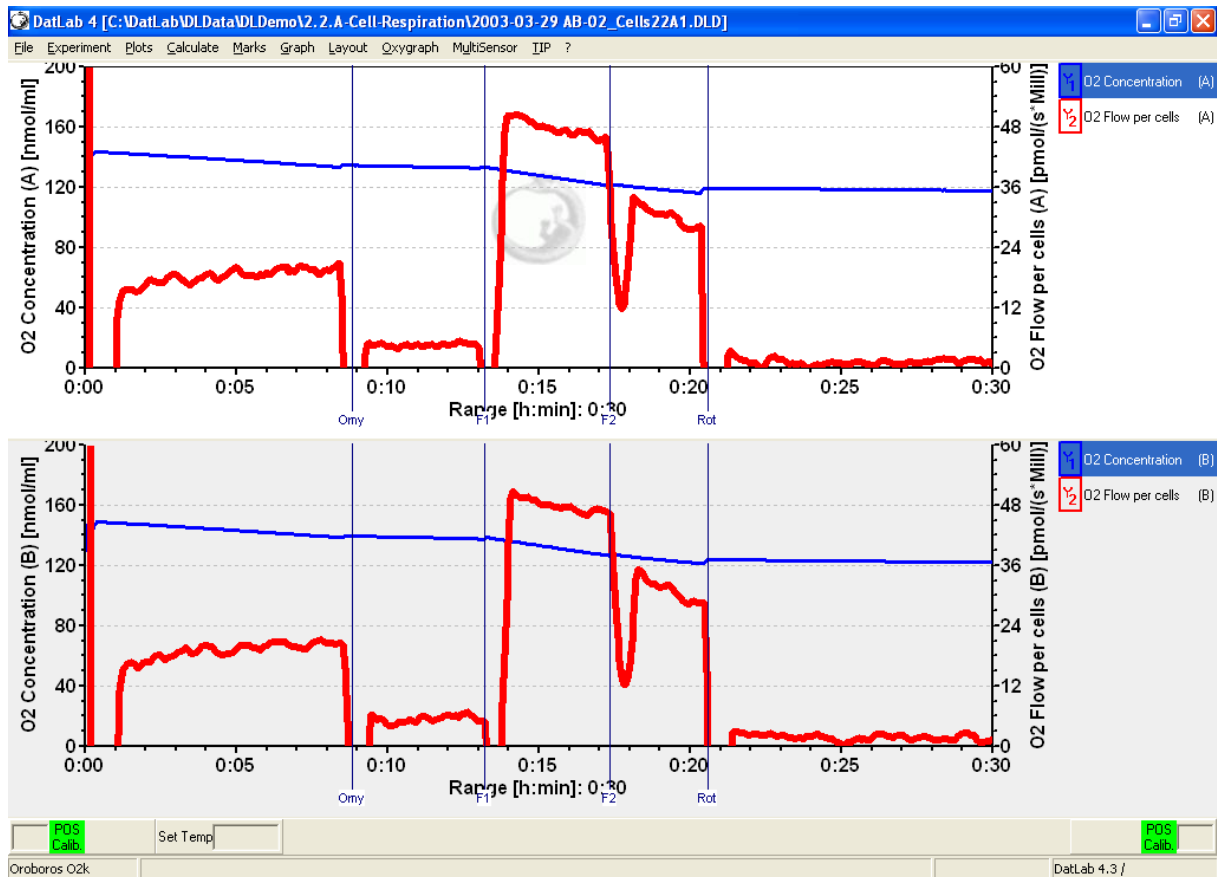


**Figure 2.** Screen shot from the experiment with lymphoblastoma cells suspended in cell culture medium (RPMI). Parallel replicate experiments in the two O2k chambers, top and bottom graph for left (A) and right chamber (B), respectively, over a 30 min period. Thin lines (blue): oxygen concentration [ $\mu\text{M}$ ]; thick lines (red): oxygen flux per volume [ $\text{pmol}\cdot\text{s}^{-1}\cdot\text{ml}^{-1}$ ] corrected for instrumental background. Vertical lines are events for additions of oligomycin (Omy: 2  $\mu\text{l}$ ; 2  $\mu\text{g}/\text{ml}$ ), reducing respiration to LEAK state (inhibition of ATP synthase); FCCP (F1: 1  $\mu\text{M}$ ; 2  $\mu\text{l}$ ), stimulating respiration to the non-coupled state of the ETS; a second FCCP titration (F2: 2  $\mu\text{M}$ ) illustrates inhibition by excess uncoupler concentration; and inhibition by rotenone (Rot: inhibitor of complex I; 5  $\mu\text{l}$ ; 2.5  $\mu\text{M}$ ). Sections are marked for calculation of average flux and export into a table of results. Note some salient features of high-resolution respirometry: Low respiratory activities (small changes of oxygen concentration over 20 min) yield highly reproducible information on oxygen flux in the two chambers. Even inhibited flux (rotenone) is measured with high reproducibility and stability.

### 2.3. Net ROUTINE flux control ratio, netROUTINE/ETS (netR/E)

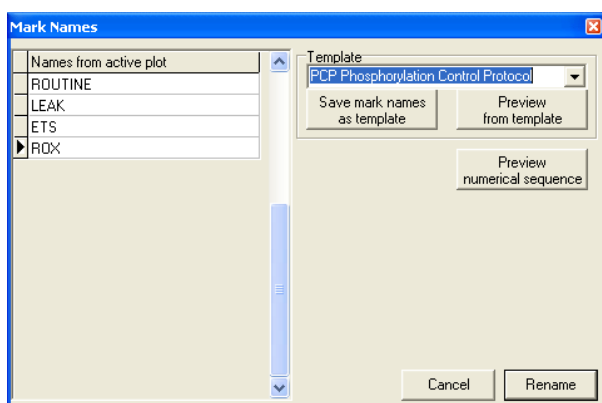
netR/E is introduced as an index which expresses phosphorylation-related respiration (ROUTINE-LEAK) as a function of non-coupled ETS capacity. netR/E remains constant, if partial uncoupling is fully compensated by an increased ROUTINE respiration rate and a constant rate of oxidative phosphorylation is maintained (Hütter et al 2004). Upon stimulation of OXPHOS, or if the respiratory capacity declines without effect on the rate

of OXPHOS, however,  $\text{net}R/E$  increases, which indicates that a higher proportion of the maximum capacity is activated to drive ATP synthesis.  $\text{net}R/E$  declines to zero in either fully uncoupled (non-coupled) cells or in cells under complete metabolic arrest. All fluxes in Eqs.(1)-(3) should be corrected for non-mitochondrial respiration, estimated after inhibition of mitochondrial respiration,  $J_{\text{ROX}}$ .

### 3. The O2k-Workshop experiment

The OROBOROS Oxygraph-2k was operated at 37.0 °C with 2 ml volume in both chambers. The stirring speed was set at 750 rpm in both chambers, using PEEK (comparable to the new standard PVDF) stirrers, and the data sampling interval was set at 2 s.

The main experiment on cellular respiration (run 1) starts after calibration of the polarographic oxygen sensors (sensor calibration), and instrumental background controls used for instrumental calibration (chamber calibration; DatLab file: [2003-03-29 O2k1-01\\_Calib\\_0809.DLD](#); [Supplement](#)).



The medium used for calibration was siphoned off the glass chamber, and 2.2 ml of the cell suspension was pipetted into each chamber, with the tip of the syringe held onto the wall of the glass chamber while the stirrers remained in continuous rotation. Culture media with FCS must be handled with particular care to avoid any generation of foam and inclusion of

bubbles when inserting the stopper. Before closing the chamber, the cell suspension was stirred for about 2 min in contact with air for oxygenation, while subsamples may be taken for cell count and enzymatic determinations. After closing the chambers, a 5- to 10-min period is required for signal stabilization, as seen in the traces of oxygen flux (Figure 2; thick lines in red). By comparison, the direct signal of oxygen concentration reveals limited visual information (Fig. 2; thin lines in blue).

Titration were performed as described in the protocol and corresponding events indicate the various titrations (Fig. 2). For each respiratory state, sections of stable flux are marked. After the second titration of

FCCP, instability of oxygen flux is due to progressive inhibition of cellular respiration by an excess concentration of the uncoupler. A prolonged period of rotenone-inhibited respiration is shown to demonstrate the instrumental stability.

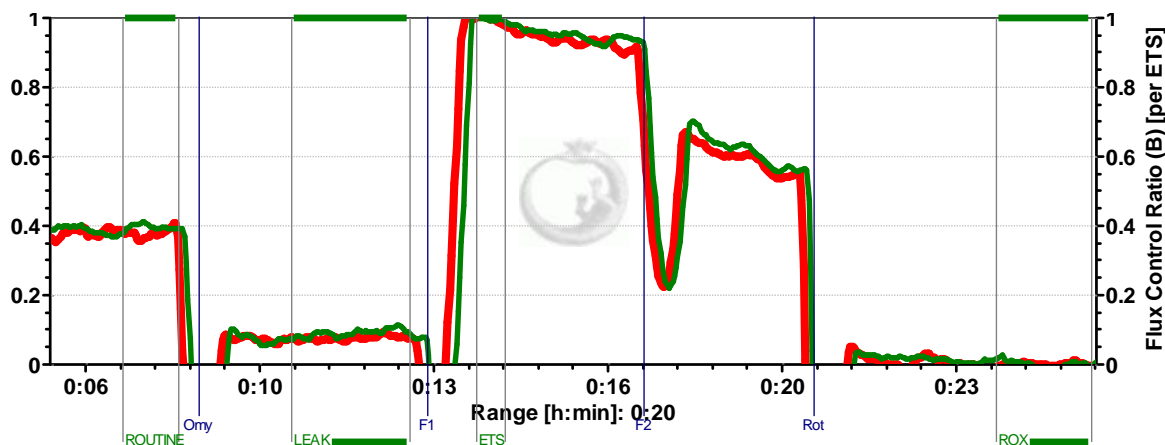








**Figure 3.** Flux control ratios ( $FCR$ ) normalized to state ETS ( $E$ ) in chambers A and B. ROUTINE respiration in these cells is regulated at 0.39 of ETS capacity ( $R/E$ ). Oligomycin ( $Omy$ ) inhibits respiration to 0.08 ETS capacity ( $L/E$ ).

**Table 1.** (a) Volume-specific respiratory flux of leukemia cells [ $\text{pmol O}_2 \cdot \text{s}^{-1} \cdot \text{ml}^{-1}$ ] after correction for instrumental background. (b) ROUTINE flux control ratios,  $R/E$  (ratio of ROUTINE and non-coupled respiration), LEAK flux control ratios,  $L/E$  (ratio of oligomycin-inhibited and non-coupled respiration), and  $ROX/E'$  ratio ( $E'$  not corrected for ROX).

a	Chamber	ROUTINE	LEAK	ETS	ROX
	A	18.68	3.74	49.35	0.89
	B	19.26	4.41	48.49	1.35
	Average	18.97	4.07	48.92	1.12
b	Chamber	$R/E$	$L/E$		$ROX/E'$
	A	0.38	0.08	1	0.02
	B	0.40	0.09	1	0.03
	Average	0.39	0.08	1	0.02

The corresponding RCR of 12 ( $=E/L$ ; Table 1) represents a state of coupling comparable to carefully isolated mitochondria. The UCR of 2.6 agrees with published uncoupling control ratios in these cells studied in mitochondrial medium (Renner et al 2003), in endothelial cells (Steinlechner-Maran et al 1996) and fibroblasts (Hütter et al 2004). This UCR indicates a high apparent respiratory excess capacity in human cells measured under physiological conditions. The net ROUTINE respiratory control ratio was 0.30 (Eq. 3), indicating that 30% of ETS capacity is utilised for phosphorylation.

## 4. References

- Gnaiger E (2008) Polarographic oxygen sensors, the oxygraph and high-resolution respirometry to assess mitochondrial function. In: Mitochondrial Dysfunction in Drug-Induced Toxicity (Dykens JA, Will Y, eds) John Wiley:327-52. » 
- Gnaiger E (2014) Mitochondrial pathways and respiratory control. An introduction to OXPHOS analysis. 4th ed. Mitochondr Physiol Network 19.12. OROBOROS MiPNet Publications, Innsbruck:80 pp. » 
- Gnaiger E, Steinlechner-Maran R, Méndez G, Eberl T, Margreiter R (1995) Control of mitochondrial and cellular respiration by oxygen. J Bioenerg Biomembr 27:583-96. » 
- Hütter E, Renner K, Pfister G, Stöckl P, Jansen-Dürr P, Gnaiger E (2004) Senescence-associated changes in respiration and oxidative phosphorylation in primary human fibroblasts. Biochem J 380:919-28. » 
- Renner K, Amberger A, Konwalinka G, Gnaiger E (2003) Changes of mitochondrial respiration, mitochondrial content and cell size after induction of apoptosis in leukemia cells. Biochim Biophys Acta 1642:115-23. » 
- Steinlechner-Maran R, Eberl T, Kunc M, Margreiter R, Gnaiger E (1996) Oxygen dependence of respiration in coupled and uncoupled endothelial cells. Am J Physiol 271:C2053-61. » 



» [MiPNet19.01D](#). O<sub>2</sub> calibration.

» [MiPNet19.01E](#). Oxygen flux analysis.



DatLab Files and Excel Templates



» [Files Protocols\MiPNet08.09 Cell-Respiration](#)

» [MiPNet06.03](#) POS calibration SOP.

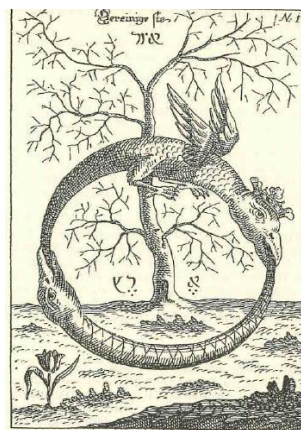
» [MiPNet14.06](#) Instrumental background and accuracy of oxygen flux.

**Supplementary information** on the workshop experiment, including calibration of oxygen concentration, instrumental background calibration and evaluation of respirometric measurements with a perspective of high-resolution respirometry is summarized in the appended sections.



**Full version: go Bioblast**

» [www.bioblast.at/index.php/MiPNet08.09\\_CellRespiration](http://www.bioblast.at/index.php/MiPNet08.09_CellRespiration)





## Supplement: Cell respiration, calibration and background correction

### A.1. Air calibration and oxygen consumption by the POS

#### A.1.1. Calibration

##### **O2k-SOP:** [MiPNet06.03 POS-Calibration-SOP](#)

For calibration and instrumental background experiments without cells, (i) air saturation is achieved in the aqueous solution by equilibration of the stirred medium with a gas phase. (ii) Instrumentally-induced rates of change of oxygen concentration over time are recorded in the closed chambers at various oxygen concentrations (Fig. 4). After chemical sterilization (70% ethanol for 20 min in the stirred chambers) and simultaneous temperature equilibration of the oxygraph (37 °C), the chambers are washed three times with distilled water, and filled with medium. The first calibration phase involves stabilization of the signal with a gas phase (air; avoiding any oxygen depletion from the calibration gas) above the stirred medium (Fig. 4, top panel A'). Signal stabilization is observed while applying initial default calibration parameters. A mark is set (Mark [R1](#)) delineating the period of a stable signal at air saturation (Fig. 4A and B; a zoom is shown in Fig. 4A').

The Oxygraph-2k records automatically with DatLab the experimental temperature and actual barometric pressure, receiving these signals continuously from the Oxygraph-2k. The average raw signal of the oxygen sensor [V], temperature and barometric pressure are displayed, by opening the DatLab Calibration window and selecting Mark [R1](#) for air calibration (Fig. 4C). The barometric pressure was 86.9 kPa or 652 mmHg (Fig. 4C) at the altitude of 1400 m in Schröcken. The oxygen solubility factor of physiological NaCl solution at 37 °C is entered as 0.92 (Fig. 4C). The oxygen concentration at air saturation, 37 °C, local barometric pressure and at 92% of the solubility of pure water, therefore, is calculated by DatLab for calibration as 164.1 µM. By comparison, air saturation at 37 °C and 100 kPa barometric pressure yields a partial oxygen pressure of 19.63 kPa for moist air, and at an oxygen solubility for pure water of 10.56 µM/kPa the standard concentration at air saturation is 207.3 µM. For culture medium (RPMI) we use an oxygen

solubility factor (oxygen solubility relative to pure water) of 0.89, yielding an air saturation concentration of 158.7  $\mu\text{M}$  for calibration. All these calculations are performed automatically by DatLab.

### A.1.2. Oxygen signal and oxygen consumption

The raw signals of the oxygen sensors were 8.55 V and 7.71 V, as displayed for the marked calibration sections. Zero oxygen calibrations have been performed before, and the value of 0.025 V was entered into the line for zero calibration. These boundary conditions resulted in calibration factors of 19.24 and 21.35  $\mu\text{M}/\text{V}$  for the right and left chamber, respectively (average 20.3), at the gain setting of 4 (corresponding to a sensor current of c. 1  $\mu\text{A}/4\text{ V}$ ). The sensor output is, therefore, approximately  $(1\ \mu\text{A}/4\text{ V}) \cdot (1\text{ V}/20.3\ \mu\text{M}) = 0.012\ \mu\text{A}/\mu\text{M}$ . Based on the stoichiometry of 4 electrons per  $\text{O}_2$  reduced at the cathode and the Faraday constant, oxygen consumption is expected at  $2.591\ \text{pmol}\ \text{O}_2 \cdot \text{s}^{-1} \cdot \mu\text{A}^{-1}$ . At air saturation (164.1  $\mu\text{M}$ ), this yields an oxygen consumption of the sensor of  $2.592 \cdot 0.012 \cdot 164.1 = 5.2\ \text{pmol}\ \text{O}_2 \cdot \text{s}^{-1}$ . In the 2 ml chamber, therefore, the expected oxygen consumption by the sensor was  $2.6\ \text{pmol}\ \text{O}_2 \cdot \text{s}^{-1} \cdot \text{ml}^{-1}$  under the specific conditions of this experiment. This corresponds to the average instrumental background oxygen consumption measured in the Oxygraph-2k at air saturation, whereas the background measured during the workshop was slightly elevated (by  $<1\ \text{pmol}\ \text{O}_2 \cdot \text{s}^{-1} \cdot \text{ml}^{-1}$ ; Fig. 4A and B).

## A.2. Instrumental background

### A.2.1. Background experiment

**O2k-SOP:** [MiPNet14.06 InstrumentalBackground](#)

Oxygen consumption of the polarographic oxygen sensor declines as a linear function of the oxygen signal, reaching zero at zero oxygen pressure. At low oxygen pressure, back-diffusion of oxygen into the chamber compensates for or dominates over oxygen consumption by the sensor. An instrumental background test, therefore, is required to determine the oxygen dynamics in the instrument at various oxygen levels. The instrumental background test was performed during the morning-presentation of the workshop, which explains the long duration (3.5 hours; Fig. 4) compared to a standard test completed within  $<2$  hours.

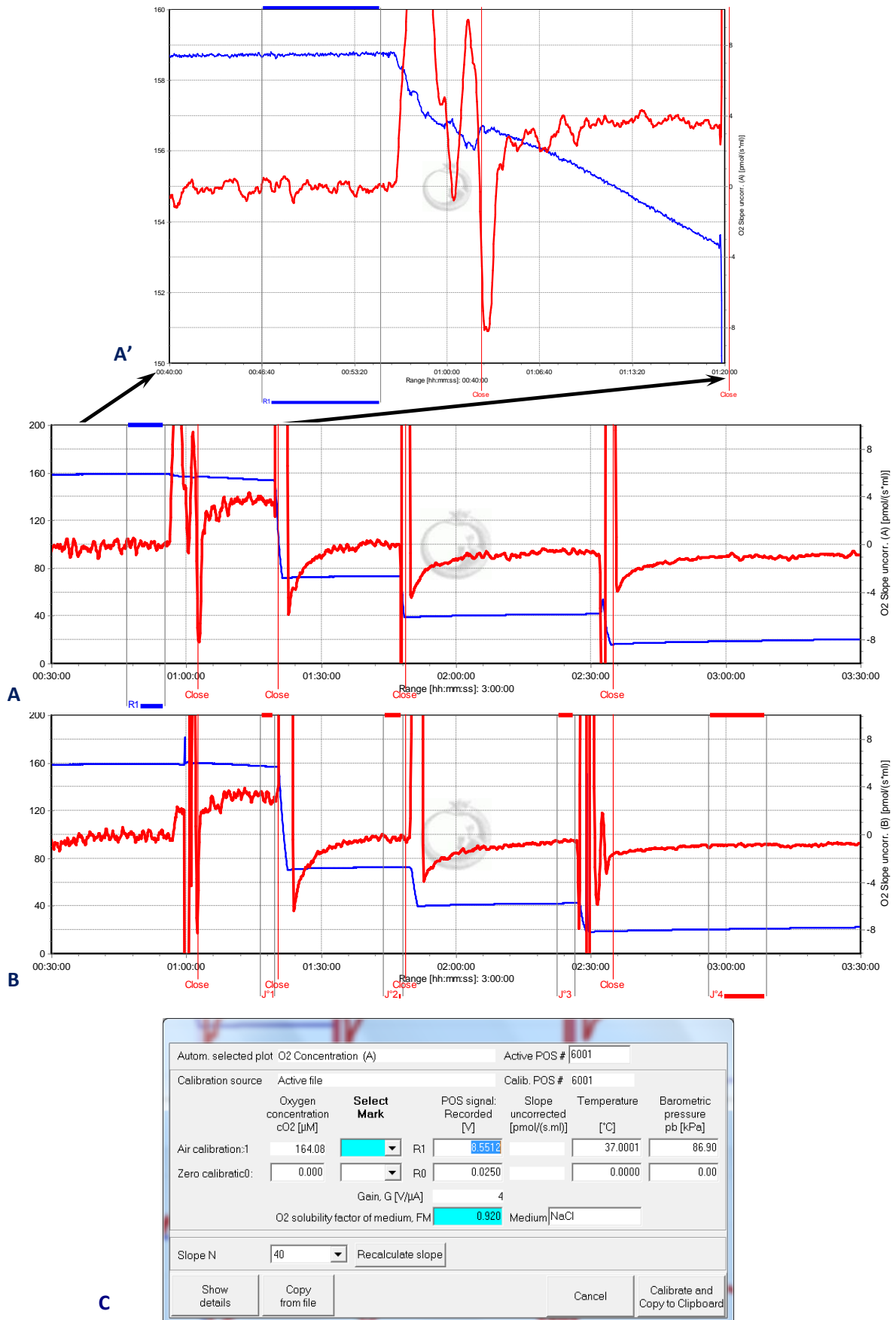


**Figure 4.** Air calibration and instrumental background control experiment: Overview of the calibration experiment (A and B for left and right chamber; A' a zoom into the calibration phase). The section of air saturation is marked (Mark R1 in A, yielding calibration information in panel C). Subsequently, instrumental

background calibration is performed at four levels of oxygen concentration (marked sections shown in Fig. B). Experimental fluxes are shown without background correction ( $O_2$  Slope uncorr.).

The linear dependence of background oxygen flux from oxygen concentration is described as the intercept at zero oxygen concentration (maximum back-diffusion of oxygen) and the slope, which are typically c.  $-2 \text{ pmol } O_2 \cdot s^{-1} \cdot ml^{-1}$  for the intercept, and 0.025 for the slope. High accuracy of respiratory flux measurement requires instrumental calibration, background control experiments and corresponding corrections performed automatically by the software DatLab.

### A.2.2. Background correction of respiratory flux

The effect of instrumental background correction is small for non-coupled respiration (<5%), increases for ROUTINE and LEAK (12 and 47%, respectively), and becomes dominating in ROX measured at high oxygen concentration (170%; Table 2 and Fig. 5). Whereas ROX was 5% of ROUTINE flux, this would be estimated at 13% with a neglect of instrumental background correction.

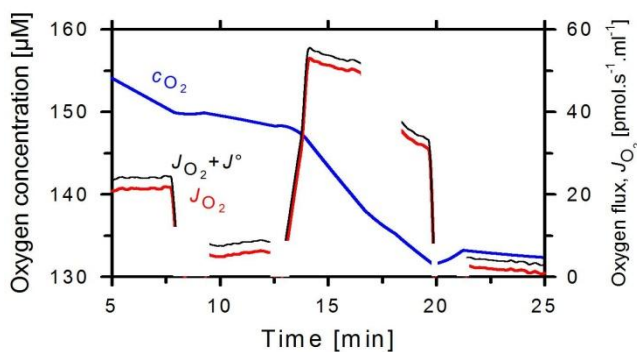


**Figure 5.** Cell respiration corrected for instrumental background oxygen flux (oxygen flux per chamber volume,  $J_{O_2}$ ; red line), compared to total oxygen flux including instrumental background ( $J_{O_2} + J^0$ ; black thin line, uncorrected). Due to low volume-specific respiratory rates, the decline of oxygen concentration was small during the experiment (left axis, amplified

from 130 to 160  $\mu\text{M } O_2$ ; blue line), and the oxygen-dependent background correction is nearly constant.

High-resolution respirometry enables flux to be resolved at small changes of oxygen concentration over time (Fig. 5). When oxygen concentrations remain high, then the background correction is dominated by the oxygen consumption of the sensor. At a steeper decline of oxygen concentration, the sign of the background correction would change, when oxygen back-diffusion predominates over sensor oxygen consumption. In this case, an initial over-estimation of respiration would change to a final underestimation. In respirometers with teflon stirrers and unappropriate sealings, the uncorrected rotenone respiration frequently appears as an increase of oxygen concentration over time.

### A.3. Optimum chamber volume, resolution of flux, and instrumental background

Respiratory flux per volume increases 10-fold when using a 10-fold lower chamber volume with the same amount of biological material, thus obtaining a 10-fold higher cell density. Would reduction of the chamber volume, e.g. to 200  $\mu\text{l}$  instead of 2 ml, reduce the background effect? The simple answer is no, since (i) the oxygen consumption rate of the oxygen sensor is independent of chamber volume, whereas the volume-specific oxygen consumption increases in indirect proportion to the chamber volume. Thus the ratio of instrumental background and biological respiration remains unchanged, whereas the complications of handling microvolumes increase as chamber volume is reduced.

**Table 2.** Apparent volume-specific respiratory flux of leukemia cells [ $\text{pmol O}_2 \cdot \text{s}^{-1} \cdot \text{ml}^{-1}$ ], uncorrected for non-mitochondrial respiration (compare Tab. 1); with correction for instrumental background (A) and without background correction (B).

	File - Chamber	ROUTINE'	LEAK'	ETS'	ROX
a	2003-03-29 A-1	19.57	4.62	50.24	0.89
	2003-03-29 B-1	20.61	5.76	49.83	1.35
	Average	20.09	5.19	50.04	1.12
Chamber					
b	2003-03-29 A-1	22.16	7.18	52.69	2.93
	2003-03-29 B-1	22.85	7.97	51.95	3.10
	Average	22.51	7.57	52.32	3.02

A more detailed analysis of the optimum chamber volume must take into account (ii) the rapid decline of oxygen concentration, leaving little scope for any tests of respiratory stability over time and multiple titrations; and (iii) the effect of back-diffusion of oxygen. This effect of back-diffusion increases with the ratio of surface area (where diffusion takes place) to chamber volume, hence micro-chambers are more problematic in terms of oxygen leakage into the system when compared to large chamber volumes. Paradoxically, the well appreciated advantages of micro-volume chambers for high-resolution of oxygen flux when biological material is limiting, are more than offset by the increasingly dominating artefacts which remain largely ignored.

Taken together, the present experimental example illustrates the advantages of high-resolution respirometry for routine applications in cellular and mitochondrial physiology.

## A.4. Graph layouts applied

Graph Layout: **"06 Specific flux per unit sample"**

For each chamber 'O2 concentration' and 'O2 flux per unit' is displayed, where unit is the unit selected in the 'Edit experiment' window. If, e.g. mg was selected, the title of the plot is 'O2 flux per mass'. The amount of sample (as mg, mill cells, or units) has to be correctly set in the 'Edit experiment' window [F3], otherwise wrong results will be displayed.

Graph Layout: **"06.MiPNet08.09 Specific flux per unit sample"**

Specific layout for demo file: [2003-03-29 O2k1-02\\_Cells\\_0809.DLD](#)

Ref: Renner K, Amberger A, Konwalinka G, Gnaiger E (2003) Changes of mitochondrial respiration, mitochondrial content and cell size after induction of apoptosis in leukemia cells. *Biochim. Biophys. Acta* 1642: 115-123.

Info: » <http://www.bioblast.at/index.php/O2k-Protocols>

Graph Layout: **"07 Gr1-Flux Gr2-O2 Conc"**

Graph 1: Display of O2-flux for both chambers.

Graph 2: Display of O2-concentration for both chambers.

The fluxes of both chambers can be directly compared in one window, while both O2 concentrations are plotted in the second window.

Manual: [O2 flux analysis](#)

[MiPNet19.01E](#)

O2k-Demo: High-resolution respirometry with leukemia cells: Respiratory control and coupling. See [\2.Protocols\MiPNet08.09](#).

Ref: Gnaiger E (2008) Polarographic oxygen sensors, the oxygraph and high-resolution respirometry to assess mitochondrial function. In: *Mitochondrial Dysfunction in Drug-Induced Toxicity* (Dykens JA, Will Y, eds) John Wiley:327-52. (see Fig.2)

Graph Layout: **09 Flux control ratios**

Before selecting this layout, define the reference and baseline metabolic states in the menu "Plots\Flux Control Ratios". Plot of flux control ratios (*FCR*) for both chambers in a single graph (Graph 1). The range for the Y axes is set to 1.0. Oxygen concentration is plotted in Graph 2 for both chambers.

Manual: [O2 flux analysis](#)

[MiPNet19.01E](#)

O2k-Demo: [Coupling control protocol with intact cells.](#)  
[An experiment of HRR with intact cells.](#)

[MiPNet08.09.](#)

[MiPNet10.04.](#)

Ref.: Gnaiger E (2008) Polarographic oxygen sensors, the oxygraph and high-resolution respirometry to assess mitochondrial function. In: *Mitochondrial Dysfunction in Drug-Induced Toxicity* (Dykens JA, Will Y, eds) John Wiley:327-52. (see Table 1)

Gnaiger E (2009) Capacity of oxidative phosphorylation in human skeletal muscle. New perspectives of mitochondrial physiology. *Int J Biochem Cell Biol* 41: 1837-45.

